Boiling of an Emulsion in a Yield Stress Fluid

Geoffroy Guéna, Ji Wang, Jean-Baptiste d'Espinose, François Lequeux, Laurence Talini

Boiling of an emulsion in a yield stress fluid

Geoffroy Guéna,* Ji Wang, Jean-Baptiste d'Espinose, François Lequeux, and Laurence Talini†
Université Pierre et Marie Curie–Paris 6, UMR CNRS 7615, Laboratoire PPMD, ESPCI, F-75005 Paris, France

We report the boiling behavior of pentane emulsified in a yield stress fluid, a colloidal clay (Laponite) suspension. We have observed that a superheated state is easily reached: the emulsion, heated more than 50 °C above the alkane boiling point, does not boil. Superheating is made possible by the suppression of heterogeneous nucleation in pentane, resulting from the emulsification process, a phenomenon evidenced decades ago in studies of the superheating of two phase fluids. We have furthermore studied the growth of isolated bubbles nucleated in the emulsion. The rate of increase of the bubble radius with time depends on both the temperature and emulsion volume fraction but, rather unexpectedly, does not depend on the fluid rheology. We show that the bubbles grow by diffusion of the alkane through the aqueous phase between liquid droplets and bubbles, analogously to an Ostwald ripening process. The peculiarity of the process reported here is that a layer depleted in oil droplets forms around the bubble, layer to which the alkane concentration gradient is confined. We successfully describe our experimental results with a simple transfer model.

I. INTRODUCTION

Liquids may be heated to temperatures far above their boiling points: superheats larger than 100 °C have been currently reported in pure liquids such as water or linear alkanes [1]. It is well known that reaching a superheated metastable state is made possible by, for instance, dispersing the liquid in another, less volatile, liquid [1,2]. The volatile dispersed phase is then isolated from the rough solid surfaces containing gas nuclei; furthermore, the impurities that are poorly wetted by the volatile phase and may thus act as boiling centers are rejected in the dispersing phase. As a result, heterogeneous nucleation is suppressed, and, for instance, superheating of pentane drops in an immiscible fluid up to 150 °C has been reported, without any special care taken to clean liquids [1]. When boiling finally occurs, vaporization can be explosive [3] and is supposedly at the origin of substantial damages in industrial processes or catastrophic volcanic eruptions.

The growth of bubbles in complex fluids is involved in industrial processes, such as polymer foaming [4]. Knowledge of the mechanisms at stake is also needed to understand phenomena ranging from the decompression sickness to volcanic eruptions. It has been shown that if the continuous phase surrounding the volatile phase presents a complex rheology, the growth of bubbles can be hampered or substantially slowed down [5–7]; the rheological properties at stake are, for instance, very high viscosities and/or elasticity. In the high elasticity case, the bubble growth (or dissolution) process can be controlled by the viscoelastic properties of the surrounding medium, leading to characteristic growth (or dissolution) times that can be one order of magnitude larger than in a Newtonian fluid [6,8]. However, quantitative characterization of bubble growth is rendered difficult by its coupling with bubble rise [7] since both phenomena potentially depend on the surrounding fluid's rheology.

Herein we study bubble growth in a complex fluid in which the bubbles remain at a fixed position. The system consists in pentane emulsified in an aqueous colloidal clay suspension, which is a transparent yield stress fluid. One specificity of this system is that the alkane droplets remain well dispersed in the aqueous phase without any added surfactant; we have shown in a previous work [9] that the droplets are prevented from coalescing or creaming simply because they are immobilized in the yield stress fluid. In particular, we have demonstrated that the adsorption of clay particles at o/w interfaces is not at the origin of the droplet stabilization: alkane emulsions in aqueous clay suspensions are therefore not Pickering emulsions. In the present work, we show that such emulsions can be heated far above the boiling point of pentane without boiling, as a result from a kinetic stabilization of liquid alkane. In addition, we study the growth of isolated bubbles, nucleated in those emulsions. Owing to the yield stress of the surrounding phase, the position of the bubbles remains fixed in the clay suspension for time lapses as large as 1 h. We show that the very slow growth process is controlled by the diffusion of the solubilized alkane toward the bubble, as in an Ostwald ripening process, and not by the rheological properties of the aqueous phase. We model the bubble growth in that frame, and the predicted variation laws are in excellent agreement with the experimental data.

In the following, we first describe the experimental system. We further report macroscopic observations of the boiling of the emulsions. The growth of bubbles nucleated from alkane drops is the object of a third part and, in Sec. V, we present a simple transfer model that successfully accounts for the experimental data.

II. EXPERIMENTAL MATERIALS AND METHODS

The yield stress fluid is an aqueous suspension of a synthetic hectorite clay, Laponite (RD, Rockwood). The suspen-

*Present address: Université Rennes I, UMR CNRS 6626, F-35000 Rennes, France.
†Corresponding author; laurence.talini@espci.fr

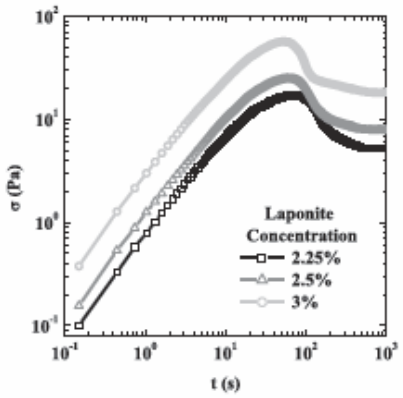

FIG. 1. Stress as a function of time measured in the Laponite suspensions of different concentrations during strain rate step experiments. The strain rate is set at 5×10^{-3} s^{-1} and the temperature at 70 °C.

sions are prepared by mixing a given amount of the Laponite powder with a sodium hydroxide aqueous solution (concentration of $10^{-4}M$). Once hydrated, the Laponite platelets have a radius of 30 nm and a height of 1 nm. Three concentrations of Laponite have been used: 2.25%, 2.5%, and 3% *w*/*w*. The suspensions are strongly stirred during one week and further kept at rest for one more week to ensure full dispersion of the Laponite platelets.

Within our experimental conditions, the Laponite suspensions form transparent, viscoelastic, yield stress fluids that are in a metastable state and thus age. In particular, their rheological properties evolve over time: both their yield stress and complex viscosity increase [10]. We estimate the yield stress values of the suspensions by performing stress measurements at a constant strain rate with an ARES rheometer. To minimize wall slip and other flow heterogeneities, the rheometer was equipped with a six bladed vane rotating in a cylinder with inner diameter of 34 mm. Since the Laponite rheological properties depend on its history, special care was taken to reproduce conditions similar to the one for the bubble growth experiments: Laponite was strongly sheared and further poured in the apparatus cylinder. To prevent evaporation, a silicone oil slick was formed on the upper surface of Laponite. Rheological measurements were conducted after a 12 h rest: the sample was first heated at 70 °C and a constant shear rate of 5×10^{-3} s^{-1} was then applied to the sample. The recorded stress vs time variations are shown in Fig. 1. Whatever the Laponite concentration, the rheological curves all exhibit a maximum, and the value of that maximum stress provides an estimate of the yield stress. We measure yield stresses of 17, 25, and 57 Pa for concentrations of 2.25%, 2.5%, and 3% *w*/*w*, respectively. Those values are similar to the ones measured at room temperature found in the literature [11,12]. As pointed out in other works [13,14], the rheological properties strongly vary with the Laponite concentration in the encompassed range.

The alkane is *n*-pentane (Chromasolv, Sigma-Aldrich), whose relevant properties are gathered in Table I, together with the used notations. Its solubility and coefficient diffusion are the ones measured in water. Our previous study suggested that the presence of the Laponite platelets does not significantly modify those values [9]. The values of the different properties at the temperatures of our experiments are not all available in the literature. In particular, the variations with temperature of the pentane molecular diffusion coefficient have been poorly documented. We indicate in Table I the numerical values we have used in what follows; we discuss the relevancy of our numerical results in Sec. VI of the paper.

Emulsions are prepared by mixing the desired amount of pentane with the Laponite suspension which is emulsified using an ultrasonic device. The pentane volume fraction has been varied from 1% to 10%. The Laponite suspension is degassed using a vacuum pump prior to emulsification; most of the gas nuclei are therefore suppressed from the aqueous phase. Owing to the strong shear exerted during the emulsification process, the Laponite suspension turns to a low-

TABLE I. Adopted notations and values of the useful thermodynamical properties of pentane found in the literature. The values used in the computations of R and ξ (see Sec. IV) appear in bold.

		T=25 °C	T=70 °C	T=90 °C
D_m [a]	Pentane molecular diffusion coefficient (m^2/s)	$(\mathbf{1.06\pm0.12})\times\mathbf{10^{-9}}$		
x^* [b]	Pentane solubility in water (mol/mol)	1.1×10^{-5}	$\mathbf{1.2\times10^{-5}}$	1.5×10^{-5}
v_L [c]	Molar volume of liquid pentane (m^3/mol)	1.16×10^{-4}	$\mathbf{1.26\times10^{-4}}$	1.31×10^{-4}
v_{H_2O} [d]	Molar volume of water (m^3/mol)	1.805×10^{-5}	$\mathbf{1.84\times10^{-5}}$	1.865×10^{-5}
γ [e]	Pentane/water interfacial tension (mN/m)	48.18		
T_b	Pentane boiling temperature		**36 °C**	
L [f]	Pentane latent heat of vaporization (J/mol)		$\mathbf{2.57\times10^4}$	
P_0	Atmospheric pressure		$\mathbf{1\times10^5}$ Pa	

[a]Reference [15].
[b]Reference [16].
[c]References [17–20].
[d]References [21,22].
[e]Reference [23].
[f]Reference [24].

viscosity liquid. After completion of the emulsification, the viscosity of the Laponite suspension at rest increases; the viscosity increase is fast enough to prevent the alkane droplets from creaming. Within a few minutes, one thus obtains an emulsion consisting of alkane droplets (typical size of 10 μm) well dispersed and immobilized in a gel-like aqueous phase.

Glass vials filled with the emulsions are placed in a silicone oil bath. Experiments have been performed at three different bath temperatures: the boiling temperature of pentane (36 °C) and two temperatures above the boiling temperature (70 and 90 °C). The former temperatures correspond to superheats above the boiling temperature of pentane of $\Delta T=34$ °C and $\Delta T=54$ °C, respectively. At room temperature, the emulsions are turbid because the alkane droplets, whose average radius is close to 10 μm, diffract light. Close to $T=70$ °C, the emulsions turn transparent because the refractive index of water and alkane become matched. The bottled emulsions are in contact with air; therefore, the emulsions remain at room pressure over the whole duration of the experiments.

For the study of bubble growth, a graphite rod (a pencil lead) is placed in the vial before it is filled with the emulsion. After a 12 h rest at room temperature, the vial is placed in the heated bath and uncorked to maintain atmospheric pressure conditions. The volume of the vial being small (6 ml), a homogeneous temperature is reached in the whole emulsion within 2 min. Bubbles are observed to nucleate on the rod typically within 20 min, and their growth is recorded using a charge-coupled device camera. The resolution is such that the smallest bubble radius measured is 50 μm. The largest measured radius is of several millimeters in a 3% Laponite suspension and can be observed within about 1 h. Above that size, the bubbles first become anisotropic in shape and start rising in the fluid, the stress resulting from the buoyancy forces getting larger than the Laponite yield stress. The data presented herein thus correspond to bubbles that are spherical and whose center remains fixed. The threshold value of the radius over which a bubble changes shape and further rises is consistent with the estimated value for the yield stress, σ^y. For that threshold value, the yield stress times the projected area of the bubble in its equatorial plane is expected to balance the buoyancy forces,

$$\sigma^y \pi R^2 = \tfrac{4}{3}\pi R^3 \Delta\rho g, \tag{1}$$

where $\Delta\rho$ is the density difference between gas pentane and Laponite ($\Delta\rho \approx 10^3$ kg m^{-3}) and g is the acceleration of gravity. A threshold radius of 5 mm corresponds to a yield stress value $\sigma^y = \frac{4}{3}R\Delta\rho g \approx 60$ Pa, which is consistent with the rheological estimations of the yield stress.

In Sec. III we will describe the behavior of pentane emulsified in the Laponite suspensions when heated above its boiling temperature.

III. SUPERHEATING AND BOILING OF THE EMULSIONS

The pentane emulsified in a Laponite suspension can be maintained in its liquid state at temperatures far above its boiling point. As illustrated in Fig. 2, no bubble appears in an emulsion at rest, heated more than 30 °C above the pentane boiling temperature. The emulsion can remain several hours without boiling. If the suspension is stirred, bubbles eventually form [Fig. 2(c)].

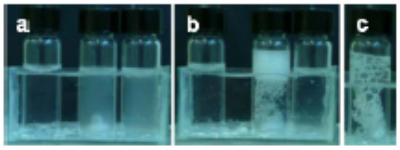

FIG. 2. (Color online) Qualitative comparison between three samples heated at different temperatures. (a) The temperature is set at the boiling temperature of pentane, $T_b=36$ °C and (b) $T=70$ °C. From left to right on each (a) and (b) photograph: the Laponite suspension without pentane, emulsion of pentane of volume fraction 5% agitated with a magnetic stirrer, and emulsion of pentane of volume fraction 5% kept at rest. (c) If the emulsion kept at rest in (a) and (b) is further stirred, the pentane boils. Note that the vial caps were not hermetically screwed; the emulsions therefore remain at atmospheric pressure.

We attribute the absence of bubbles in the emulsified pentane to a kinetic stabilization, similar to the one reported for two phase fluids in the literature [1,2]. Although no special care is taken to work with clean liquids and vials, heterogeneous nucleation is suppressed as a consequence of the emulsification process and as recalled in Sec. I.

We have checked that the boiling behavior of the emulsions does not result from a shift in the boiling temperature induced by overpressures in the alkane droplets. Overpressures originate from the capillary pressure and from the internal stresses in the surrounding elastic fluid, which exist as long as the yield criterion is not fulfilled. The capillary overpressure in a drop of radius R is given by

$$\Delta P_{cap} = \frac{2\gamma}{R}, \tag{2}$$

with γ being the water/alkane interfacial tension.

For alkane drops of radius 10 μm, the expected capillary overpressure is of the order of 10 kPa. Following the calculation detailed in Appendix A, the overpressure resulting from the internal stresses in the aqueous phase surrounding the pentane droplets is

$$\Delta P_{yield\ stress} = 2\sigma^y \ln\left(\frac{h}{R}\right), \tag{3}$$

where σ^y is the fluid yield stress and h is the depth from the air/emulsion interface at which the droplet is located.

For a depth of a few centimeters and a yield stress of 100 Pa, the corresponding overpressure is smaller than 2 kPa. The increase in the boiling temperature of the alkane, ΔT, can be related to the overpressures using the linearized form of the Clausius-Clapeyron equation,

$$\Delta T \approx \frac{(v_G - v_L)T_b}{L}\Delta P, \tag{4}$$

where L is the latent heat of the vaporization, T_b is the boiling temperature at atmospheric pressure, and v_G and v_L are

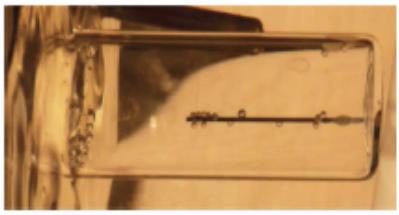

FIG. 3. (Color online) Photograph of bubbles nucleated on a graphite rod, which is immersed in an emulsion of pentane in a Laponite suspension. The vial containing the emulsion is placed in a silicone oil bath. The vial diameter is 15 mm.

the molar volumes of gas and liquid pentane, respectively. Using the numerical values given in Table I and the ideal-gas law for molar volume v_G, Eq. (4) yields temperature increases smaller than 1 °C for the computed overpressures.

In conclusion, the observed superheating of the alkane emulsified in the Laponite suspensions cannot be explained by the overpressures, originating from either capillary or yield stress effects. It must result from the suppression of heterogeneous nucleation, as previously observed in two fluid mixtures.

In Sec. IV we focus on the growth of bubbles whose nucleation has been induced in the emulsion.

IV. BUBBLE GROWTH

As described in Sec. II, we have measured the radius as a function of time of bubbles, nucleated on a graphite rod immersed in the emulsion (see Fig. 3). The vial is heated above the boiling point of pentane, and we denote as ΔT the superheat ($\Delta T = T - T_b$).

Figure 4 shows the radius of bubbles as a function of time at given temperature and pentane volume fraction in three Laponite suspensions of different concentrations.

The raw data all follow a single curve, which is well described by an increase of the radius with the square root of

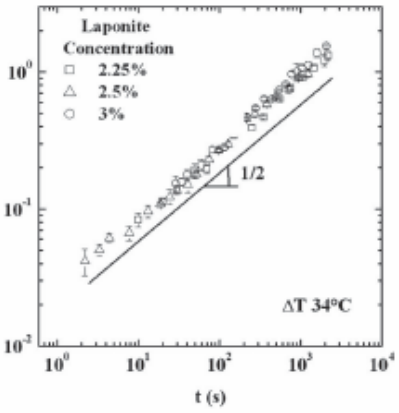

FIG. 4. Radius of isolated bubbles as a function of time and for emulsions prepared from the Laponite suspensions at three different concentrations. The alkane volume fraction ϕ is the same in all the emulsions, within the experimental uncertainty $\phi = 2.7\% \pm 0.2\%$.

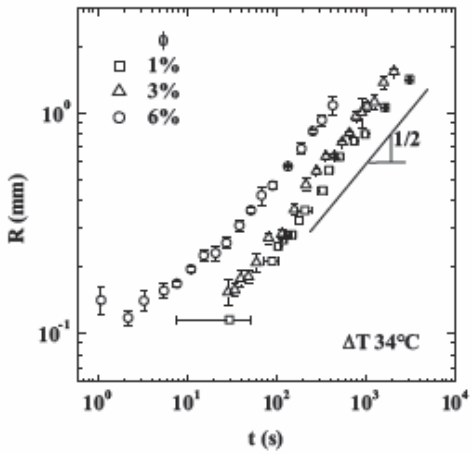

FIG. 5. Bubble radius as a function of time for different pentane volume fractions.

time, irrespective of the Laponite concentration,

$$R(t) = a\sqrt{t}. \tag{5}$$

The growth therefore proceeds regardless of the fluid yield stress or of any of the fluid rheological properties since those properties are known to strongly vary with the Laponite concentration within the range encompassed herein [11–14]. In the tested Laponite suspensions, we have indeed estimated the yield stress to vary from 17 to 57 Pa when the Laponite concentration varies from 2.25% to 3%.

The bubble growth however does depend on the pentane volume fraction of the emulsion, ϕ, as demonstrated in Fig. 5, in which we report the bubble radius variations with time for three different values of ϕ. In all cases, the increase of the radius following Eq. (5) is reached after an initial growth regime lasting ~ 10 s.

The same power-law growth of $R(t)$ is obtained at a different temperature. Figure 6 gathers the obtained values of the coefficient a defined in Eq. (5) as a function of ϕ and for two different temperatures. Although the data are somewhat dispersed, at a given temperature, a square-root variation of a with ϕ correctly describes the data. Furthermore, as the temperature increases, the bubble growth process indeed fastens and the coefficient a increases. The dependency of the growth process on volume fraction and temperature will be further discussed in Sec. V.

In summary, we have found that, after an initial transient regime, the bubble radius varies proportionally with the square root of time, with a coefficient that depends on alkane volume fraction and temperature but is independent of the surrounding fluid rheology. The bubble growth is therefore solely controlled by the transfer of alkane from the emulsion to the bubble. In Sec. V, we discuss those results in the light of a simple transfer model.

V. MODEL FOR THE BUBBLE GROWTH PROCESS

The transfer of alkane from the droplets to the bubble proceeds by diffusion through the aqueous phase. The alkane

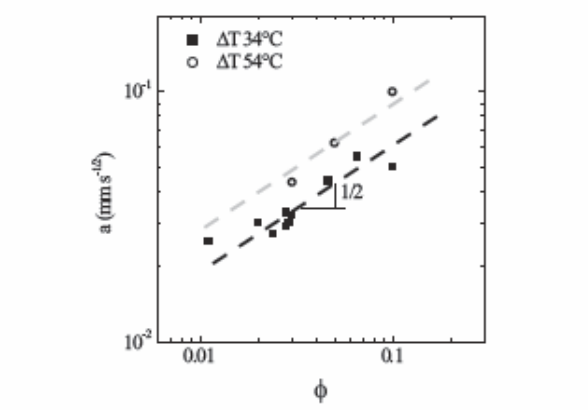

FIG. 6. Bubble growth coefficient a [defined in Eq. (5)] as a function of the pentane volume fraction in the emulsion and for two different temperatures. The dotted lines are best square root fits to the experimental data.

droplets in the vicinity of the bubble empty out first to feed the bubble and a droplet-free zone consequently forms in the aqueous phase around the bubble. The presence of that zone is evidenced in Fig. 7 that shows a close view of a bubble in the emulsion. The droplet-free zone is analogous to the one formed during the evaporation of the same emulsion in contact with air which has been the object of a previous work [9]. The evaporation is then controlled by the diffusion of the alkane through the droplet-free zone from the emulsion droplets to the atmosphere. In the present work, the bubble replaces the atmosphere.

The process of bubble growth we observe is reminiscent of the Ostwald ripening in emulsions, for which mass transfer between droplets occurs through molecular diffusion in the continuous phase [25]. In the case of the Ostwald ripening, indeed some droplets dissolve whereas others grow, and it has been shown to result in an increase with time of the droplet mean radius scaling as $t^{1/3}$, associated with a widening of the drop size distribution [25,26]. Nevertheless, the nature of the process reported herein is closer (although inverse) to the dissolution of gas bubbles in an unsaturated liquid. In the latter phenomenon, provided that surface-tension effects are negligible, a linear increase of the bubble radius with the square root of time is found in line with our experimental data. The dissolution process is classically described in the frame of the Epstein-Plesset model [27], which well captures the experimental results on dissolving gas bubbles [28]. The Epstein-Plesset model considers the diffusion of the gas in the surrounding liquid and neglects the convection term in the diffusion equation. The case of the emulsions we consider here however presents one difference: the presence of alkane droplets surrounding the bubble and constituting reservoirs of alkane. Whereas in the problem of gas dissolution, described with the Epstein-Plesset model, the concentration gradient extends in a zone of size R, it is confined within the droplet-free zone in the emulsions we deal with. As shown in the following, the size of that zone remains smaller by one order of magnitude than the bubble radius.

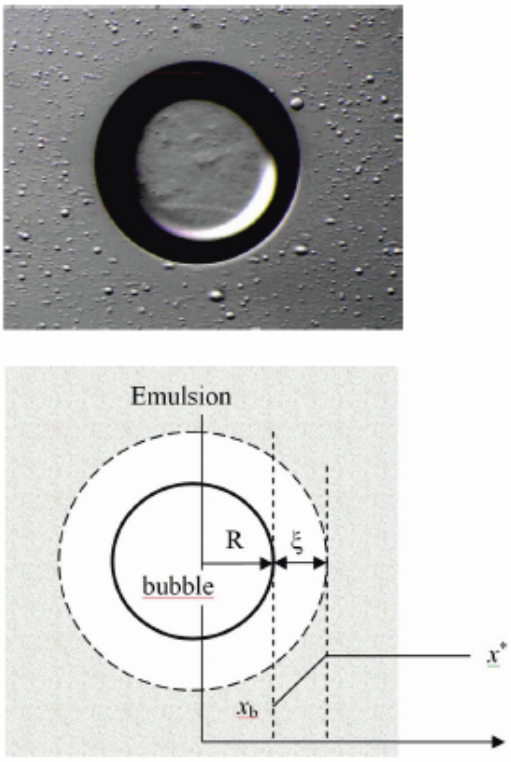

FIG. 7. (Color online) (a) Photograph of a bubble (diameter of 150 μm) quenched between two microscope slabs. The two-dimensional geometry allows us to evidence a droplet-free zone formed around the bubble. (b) Schematic representation of the bubble and its droplet-free zone of thickness ξ over which the alkane concentration gradient is confined.

Finally, let us note that bubble formation has been studied in systems similar to ours, the so-called phase-change emulsions [29]. In those systems, a volatile emulsified material changes from a liquid to a gas upon heating, which, e.g., favors the propagation of sound waves through the emulsion and has numerous applications. However, the existing works on those systems have focused on the volume change of the volatile phase without considering diffusion from the material dissolved in the continuous phase.

Consequently, we describe the problem as follows: the spherical bubble of radius R is surrounded by a droplet-free shell of thickness ξ, over which the solubilized alkane diffuse [see Fig. 7(b)]. We denote as x_b the alkane concentration at the shell/bubble interface and x^* the alkane solubility in the aqueous phase. In the distance between bubbles being large, we assume that the concentration of the solubilized alkane is x^* outside the shell.

The time derivative of thickness ξ writes

$$\frac{\partial \xi}{\partial t} = \frac{D}{\xi} - \frac{2\xi}{R}\frac{\partial R}{\partial t}. \qquad (6)$$

The first term of the right side of Eq. (6) corresponds to the increase of ξ by transfer of the alkane from the droplets to

the aqueous phase. It is written by analogy with the results obtained for the evaporation of emulsions [9]. We have shown that, in the latter case, the growth of the droplet-free zone that develops is diffusive and can be written as $\sqrt{2Dt}$. Coefficient D is an effective diffusion coefficient that, in particular, depends on the emulsion volume fraction and on the alkane concentration difference at the bubble/shell and emulsion/shell interfaces,

$$D = \frac{v_L}{v_{H_2O}} \frac{D_m}{\phi} (x^* - x_b) \tag{7}$$

where v_L and v_{H_2O} are the molar volumes of liquid pentane and water, respectively, D_m is the pentane diffusion coefficient in the aqueous phase, and ϕ is the pentane volume fraction in the emulsion.

The decrease of the effective diffusion coefficient with an increase of the emulsion volume fraction reflects the fact that the alkane droplets behave like reservoirs: the more droplets are concentrated in the emulsion, the slower is the growth of the droplet-free zone. Furthermore, the decrease of D with increasing pentane volume fraction results in the formation of a self-sharpening interface between the emulsion and the droplet-free zone, as discussed in our previous work [9].

The diffusive growth of thickness ξ is in competition with the decrease of ξ, accounted for by the second term of the right part of Eq. (6). That decrease is induced by the bubble growth and is therefore of convective nature; the resulting variation of ξ is obtained by writing the volume conservation of the layer of thickness ξ as radius R increases. The convective term as it is written in Eq. (6) is a result of an approximation considering $R \gg \xi$. This approximation is justified *a posteriori* (see below the discussion of Fig. 8) and results in underestimating coefficient a [characterizing the growth of R with time, as defined in Eq. (5)] by less than 1%.

As ξ varies, the bubble is fed by the alkane diffusing from the droplets and through the droplet-free zone surrounding the bubble. The resulting growth of the bubble radius R is simply described by relating the increase in the number of pentane moles in the bubble [at a rate $dn/dt = 4\pi R^2 D_m (x^* - x_b)/(\xi v_{H_2O})$] to the bubble volume increase with respect to the molar volume of pentane v_G. One finally obtains

$$\frac{dR}{dt} = \frac{C}{\xi}, \tag{8}$$

where C is given by

$$C = D_m (x^* - x_b) \frac{v_G}{v_{H_2O}} \tag{9}$$

and R and ξ are, therefore, given by the two coupled differential equations [Eqs. (6) and (8)], and their variations with time depend on the coefficients C and D given by Eqs. (7) and (9). Both coefficients are functions of the alkane concentration at the bubble/shell interface, x_b, which itself depends, among other parameters, on the temperature of the emulsion. We show in Appendix B that, using the Clausius-Clapeyron equation, x_b can be simply expressed as a function of known quantities, among which the superheat ΔT. In the frame of the approximations made in Appendix B and further discussed in the following, coefficients C and D both linearly vary with the superheat ΔT.

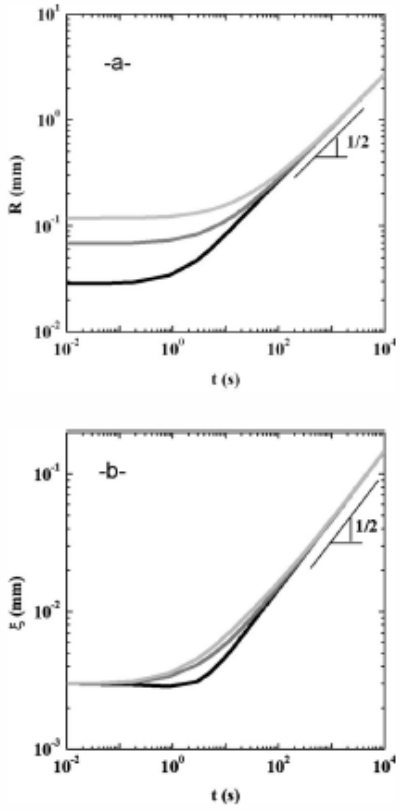

FIG. 8. Numerical resolution of the coupled differential equations [Eqs. (6) and (8)], which yields the time variations of (a) bubble radius R and (b) droplet-free zone thickness ξ for ϕ=3% and different initial bubble radii: 10 μm (black), 50 μm (dark gray), and 100 μm (light gray). The initial value of ξ is set at 0.1 nm.

We have numerically solved the differential equations [Eqs. (6) and (8)] to obtain the time variation of bubble radius R and droplet-free layer thickness ξ. Figure 8 shows those two quantities as a function of time for a set of parameters corresponding to the experiment and for different initial bubble radii. Thickness ξ (which has not been measured in three-dimensional experiments) remains smaller than the bubble radius by about one order of magnitude. It exhibits similar variations as R except for bubbles that are initially very small and for which nonmonotonic behavior of $\xi(t)$ is observed. In that case, the initial decrease of ξ results from dominating convection effects for small bubbles. After that first phase, which depends on the initial conditions, the curves merge into a single one, and the same increase with square root of time is found for both radius R and thickness ξ, whatever the initial bubble size. The duration of the first phase is on the order of 10 s, in good agreement with the experiments.

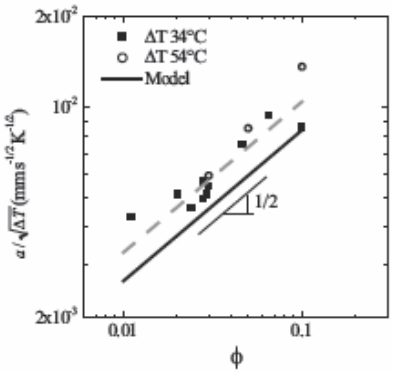

FIG. 9. Same data as Fig. 7 but shown as a plot of $a/\sqrt{\Delta T}$ as a function of the emulsion volume fraction. The experimental data (squares and circles) follow a single curve corresponding to a variation with square root of pentane volume fraction (dotted line), showing that, as expected, $a \propto \sqrt{\phi \Delta T}$. The values of $a/\sqrt{\Delta T}$ computed by numerically solving Eqs. (6) and (8) are represented by the full line curve.

The long-time solution $R(t)=a\sqrt{t}$ injected into Eqs. (6) and (8) yields for coefficient a,

$$a = C\sqrt{\frac{6}{D}}, \tag{10}$$

where C and D are given by Eqs. (7) and (9), respectively.

As shown in Appendix B, C and D can also be expressed by Eqs. (B5) and (B6); the expected variations of a with the emulsion volume fraction and the superheat are, therefore, $a \propto \sqrt{\phi \Delta T}$ in the frame of the approximations made. The first approximation consists in considering that the bubble mainly contains gas pentane, and no other gases, i.e., that the total pressure in the drop equals the pentane gas pressure. Since we carefully degas the Laponite suspensions, the quantity of dissolved gas in the aqueous phase is likely to be small. Indeed, we have observed that in nondegassed Laponite the bubbles grow faster than in degassed Laponite. The second approximation made is that the pentane saturating pressure is given by a linearized Clausius-Clapeyron equation, which is valid for small superheats: $\Delta T/T_b \ll 1$. Although relative temperature variations from the boiling temperature reach $\sim$15%, the prediction $a \propto \sqrt{\Delta T}$ resulting from these assumptions is in rather good agreement with the experimental data, as shown in Fig. 9. The experimental data of Fig. 9 are the same as in Fig. 7, but it is the quantity $a/\sqrt{\Delta T}$ that is displayed as a function of the emulsion volume fraction for two different ΔT. Considering the data dispersion, the expected collapse of the data onto a single curve is found. Therefore, $a \propto \sqrt{\Delta T \phi}$ and the approximations made are justified. In summary, the simple transfer model, together with the proposed approximations, captures well the experimental trends.

In Fig. 9, we also compare the experimental values of $a/\sqrt{\Delta T}$ to the numerical solutions of Eqs. (6) and (8). The numerical values for the properties of pentane given in Table I have been used. The agreement between numerical and experimental data is not completely satisfactory since the computed values of $a/\sqrt{\Delta T}$ are smaller than the experimental ones by about 10%. This discrepancy probably results from the value used for the pentane molecular diffusion coefficient, which has been taken at 25 °C, the data at the temperatures of the experiments missing in the literature. It remains that the trends predicted by the model are in fairly good agreement with the experiments.

VI. CONCLUSION

In conclusion, we report the boiling behavior of emulsions of pentane in aqueous yield stress fluids. First, as observed decades ago in two phase fluids, a superheated metastable state is reached when heating the emulsions at temperatures more than 50 °C above the boiling temperature of pentane. Second, we have, in addition, studied the growth of bubbles nucleated in the emulsion. Owing to the yield stress of the Laponite suspension, the bubbles are immobilized and their growth can be easily characterized. We show that it is the diffusion of alkane from droplets to bubbles through the aqueous phase that controls the growth process and not the rheological properties of the surrounding fluid. We describe the experimental data using a simple transfer model that takes into account the creation of a droplet-free zone in the aqueous phase around the bubble. The model captures well the features of the experimental results. In particular, the predicted dependency on the emulsion volume fraction and the temperature are in good agreement with the ones found experimentally.

ACKNOWLEDGMENT

We thank Vadim Nikolayev for fruitful discussions.

APPENDIX A: OVERPRESSURE IN AN ALKANE DROPLET RESULTING FROM THE SURROUNDING FLUID YIELD STRESS, DERIVATION OF EQ. (3)

We consider a cavity of radius R in a fluid with yield stress σ^Y. For the sake of simplicity, the bubble is considered to lie at the center of a sphere of the yield stress fluid, with the pressure equal to the atmospheric pressure on the surface of the sphere. Using spherical coordinates, we denote as σ_{rr}, $\sigma_{\phi\phi}$, and $\sigma_{\theta\theta}$ the nonzero components of the stress tensor. For symmetry reasons, $\sigma_{\phi\phi}=\sigma_{\theta\theta}$. We consider the mechanical equilibrium of a spherical cap of apex angle 2α, as schematized in Fig. 10.

The normal stress balance writes

$$\pi\alpha^2[(r+dr)^2\sigma_{rr}(r+dr) - r^2\sigma_{rr}(r)] = 2\pi r\alpha^2 dr\sigma_{\theta\theta}, \tag{A1}$$

which yields

$$\frac{d}{dr}(r^2\sigma_{rr}) = 2r\sigma_{\theta\theta}. \tag{A2}$$

In the fluid at rest, according to the von Mises criterion, the difference between σ_{rr} and $\sigma_{\theta\theta}$ is at most the yield stress $|\sigma_{rr}-\sigma_{\theta\theta}| \leq \sigma^Y$. We, therefore, write

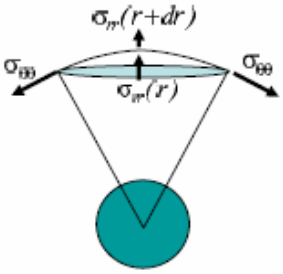

FIG. 10. (Color online) Schematic representation of the stresses on a spherical cap of apex angle 2α.

$$\sigma_{\theta\theta} = \sigma_{rr} + \sigma^Y. \tag{A3}$$

Combining Eqs. (A2) and (A3) and integrating the resulting equation yield

$$\sigma_{rr} = P(r) + 2\sigma^Y \ln\left(\frac{r}{R}\right), \tag{A4}$$

where $P(r)$ is the pressure in the surrounding medium at distance r of the distance of the cavity. A rough evaluation of the overpressure in a pentane droplet located at a vertical distance h from the air/emulsion interface is, therefore, given by

$$\Delta P = 2\sigma^Y \ln\left(\frac{h}{R}\right). \tag{A5}$$

APPENDIX B: CONCENTRATION OF PENTANE AT LAPONITE/BUBBLE INTERFACE, ESTIMATE USING THE CLAUSIUS-CLAPEYRON EQUATION

The alkane concentration at the Laponite/bubble interface x_b is related to the vapor pressure P of the alkane in the bubble using Henry's law,

$$\frac{x_b}{x^*} = \frac{P}{P_{sat}}, \tag{B1}$$

where P is the vapor pressure of pentane in the bubble, P_{sat} its saturation pressure, and x^* its solubility in water.

We assume that the bubble mainly contains gas alkane: the alkane pressure P is therefore close to the bubble pressure, which is itself given by the pressure in the surrounding fluid, taken equal to the atmospheric pressure, P_0. The saturation pressure depends on the temperature and can be related to the superheat ΔT using the Clausius-Clapeyron equation developed at the first order for small superheats, i.e., $\Delta T/T_b \ll 1$,

$$P_{sat} - P_0 \approx \frac{L\Delta T}{T_b(v_G - v_L)}. \tag{B2}$$

Equation (B2) combined with the ideal-gas law $v_G \approx R_G T_b/P_0$ and the approximation $(v_G - v_L) \approx v_G$ yields

$$P_{sat} - P_0 \approx \frac{L\Delta T}{R_G T_b^2} P_0. \tag{B3}$$

The expression for the concentration difference $x^* - x_b$ is inferred from Eqs. (B1) and (B3) and writes at the first order in $\Delta T/T_b$,

$$x^* - x_b \approx x^* \frac{L}{R_G T_b^2} \Delta T. \tag{B4}$$

Reporting Eq. (B4) in Eq. (7) yields for the effective diffusion coefficient D of the droplet-free layer,

$$D \approx \frac{v_L}{v_{H_2O}} \frac{x^* D_m}{\phi} \frac{L}{R_G T_b^2} \Delta T. \tag{B5}$$

Using Eq. (B4) and $v_G \approx R_G T_b/P_0$, the coefficient C given by Eq. (9) writes

$$C \approx \frac{x^* D_m L}{v_{H_2O} P_0 T_b} \Delta T. \tag{B6}$$

[1] M. Blander, D. Hengsten, and J. L. Katz, J. Phys. Chem. **75**, 3613 (1971).
[2] N. V. Bulanov and B. M. Gasanov, Int. J. Heat Mass Transfer **51**, 1628 (2008).
[3] J. E. Shepherd and B. Sturtevant, J. Fluid Mech. **121**, 379 (1982).
[4] C. Sagui, L. Piché, A. Sahnoune, and M. Grant, Phys. Rev. E **58**, 4654 (1998).
[5] O. Navon, A. Chekhmir, and V. Lyakhovsky, Earth Planet. Sci. Lett. **160**, 763 (1998).
[6] Y. Shimomura, T. Nishimura, and H. Sato, J. Volcanol. Geotherm. Res. **155**, 307 (2006).
[7] X. Frank *et al.*, Chem. Eng. Sci. **62**, 7090 (2007).
[8] W. Kloek, T. van Vliet, and M. Meinders, J. Colloid Interface Sci. **237**, 158 (2001).
[9] G. Guena *et al.*, Eur. Phys. J. E **28**, 463 (2009).
[10] D. Bonn *et al.*, Europhys. Lett. **59**, 786 (2002).
[11] H. Tabuteau *et al.*, EPL **78**, 68007 (2007).
[12] T. Gibaud, C. Barentin, and S. Manneville, Phys. Rev. Lett. **101**, 258302 (2008).
[13] A. Mourchid *et al.*, Langmuir **11**, 1942 (1995).
[14] S. Jabbari-Farouji, M. Atakhorrami, D. Mizuno, E. Eiser, G. H. Wegdam, F. C. MacKintosh, D. Bonn, and C. F. Schmidt, Phys. Rev. E **78**, 061402 (2008).
[15] W. S. Price and O. Soderman, J. Phys. Chem. A **104**, 5892 (2000).
[16] L. C. Price, AAPG Bull. **60**, 213 (1976).
[17] R. Span, *Multiparameter Equations of State—An Accurate Source of Thermodynamic Property Data* (Springer, Berlin, 2000).
[18] M. Jaeschke and P. Schley, Int. J. Thermophys. **16**, 1381 (1995).

[19] A. Polt, B. Platzer, and G. Maurer, Chem. Tech. (Leipzig) **44**, 216 (1992).
[20] K. E. Starling, *Fluid Thermodynamic Properties for Light Petroleum Systems* (Gulf Publishing Company, Houston, TX, 1973).
[21] W. Wagner and A. Pruss, J. Phys. Chem. Ref. Data **31**, 387 (2002).
[22] A. Saul and W. Wagner, J. Phys. Chem. Ref. Data **18**, 1537 (1989).
[23] Y. H. Mori, N. Tsui, and M. Kiyomiya, J. Chem. Eng. Data **29**, 407 (1984).
[24] William D. McCain, Jr., *The Properties of Petroleum Fluids*, 2nd ed. (PennWell Corporation, Pulsa, Oklahoma, 1990).
[25] A. S. Kabalnov, A. V. Pertzov, and E. D. Shchukin, J. Colloid Interface Sci. **118**, 590 (1987).
[26] B. P. Binks *et al.*, Langmuir **16**, 1025 (2000).
[27] S. Epstein and M. S. Plesset, J. Chem. Phys. **18**, 1505 (1950).
[28] P. B. Duncan and D. Needham, Langmuir **20**, 2567 (2004).
[29] D. R. Evans, D. F. Parsons, and V. S. J. Craig, Langmuir **22**, 9538 (2006).